Subcentimeter Tumor Lesion Delineation for High-Resolution ^{18}F-FDG PET Images: Optimizing Correction for Partial-Volume Effects

Elin Wallstén, Jan Axelsson, Torbjörn Sundström, Katrine Riklund, and Anne Larsson

Department of Radiation Sciences, Umeå University, Umeå, Sweden

In PET, partial-volume effects cause errors in estimation of size and activity for small objects with radiopharmaceutical uptake. Recent methods for image reconstruction, compared with traditional reconstruction techniques, include algorithms for resolution recovery that result in images with higher resolution and enable quantification of size and activity of smaller objects. The purpose of this study was to evaluate a combination of 2 algorithms for volume delineation and partial-volume correction on uptake volumes smaller than 0.7 mL using image reconstruction algorithms with and without resolution recovery. **Methods:** Volumes of interests (VOIs) were delineated using a threshold intensity calculated as a weighted sum of tumor and background intensities. These VOIs were used for calculating correction factors by convolving a tumor mask with the system point-spread function. The methods algorithms were evaluated using a phantom constructed from 5 small different-sized balloons filled with ^{18}F-FDG in background activity. Six different backgrounds were used. Data were acquired using a PET/CT scanner, and the images were reconstructed using 2 iterative algorithms, one of which used a resolution recovery algorithm. **Results:** For the images reconstructed using the resolution recovery algorithm, the method for volume delineation resulted in VOI sizes that were correct within 1 SD for all balloons of a volume of 0.35 mL (equivalent diameter, 8.8 mm) and larger, in all backgrounds. For the images reconstructed without resolution recovery, the VOI sizes were background-dependent and generally less accurate. Correct volume delineations generally led to accurate activity estimates. **Conclusion:** The algorithms tested on the phantom developed for this study could, for this PET camera and these reconstruction algorithms, be used for accurate volume delineation and activity quantification of lesions 0.35 mL and larger.

Key Words: PET; partial-volume effects; partial volume correction; volume delineation; resolution recovery

J Nucl Med Technol 2013; 41:85–91
DOI: 10.2967/jnmt.112.117234

PET with ^{18}F-FDG is frequently used for diagnosis and staging of tumors and for therapy evaluation (*1*). Many methods for analyzing ^{18}F-FDG uptake in tumors are quantitative or semiquantitative (*2*), and a frequently used measure is the standardized uptake value (SUV) (*3*). SUV is subject to several factors affecting its reliability, such as motion artifacts, dependence on time between injection and image acquisition, and the method used for volume delineation (*4*). In addition to these, the relatively poor spatial resolution introduces biases, especially for small objects (*5*), such as small tumors and lymph nodes. This is called the partial-volume effect (PVE) (*6*). There is a demand for more complex algorithms for correct delineation also for larger tumors (*7*), and because SUV plays an important prognostic role in many cancer studies, such as non–small cell lung cancer imaging, there is a need for correct delineation and SUV calculations (*8*). Many studies have been performed on this subject (*9–11*) for varying objects and resolution. There are also extensive reviews on the subject (*5,12*).

The spatial resolution of PET images is normally between 3.5 and 7 mm, measured as the full width at half maximum (FWHM) of the point-spread function (PSF). The relatively poor spatial resolution causes spillover between regions with different activity concentrations. PVE is often quantified with the recovery coefficient (RC)—that is, the ratio between the activity concentration measured in the image and the true activity concentration (*13*). The RCs can also be calculated theoretically and used as factors for correcting the measured activity in a volume of interest (VOI).

The SUV is often used as a measured quantity for diagnosis and staging of tumors and lymph nodes (*14,15*). Commonly, a threshold value is used as a measure of malignancy (*16*). SUV can, for example, be measured as the mean value within a VOI or a region of interest (ROI) or as the maximum voxel value within the VOI or ROI. Using the mean results in a measure that is more affected by PVE, whereas the maximum value is more sensitive to noise and typically represents an overestimation of the actual value (*17*). Both the mean and maximum values are dependent on the method used for image reconstruction, because the reconstruction method affects image noise and resolution. If proper partial-volume corrections can be performed, the threshold

Received Feb. 22, 2013; revision accepted Feb. 24, 2013.
For correspondence or reprints contact: Elin Wallstén, Department of Radiation Sciences, Radiation Physics, Umeå University, 901 87 Umeå, Sweden.
E-mail: elin.wallsten@radfys.umu.se
Published online May 8, 2013.

value for determining malignancy will be independent of the reconstruction method chosen.

Recent methods for image reconstruction, compared with traditional reconstruction techniques, include algorithms for resolution recovery that result in images with higher resolution (*18*) and enable quantification of the activity and size of smaller objects than before. Many studies of PVE have been performed using acrylic or glass phantoms with fillable spheres of different sizes (*9,10,19*). However, these spheres have walls of approximately 1-mm thickness, which creates activity-free zones and will result in an underestimation of spill-in from the background. This is problematic for the estimation of both volume and activity as has been shown in other studies. A study by Bazañez-Borgert et al. (*20*) focuses on measured RCs that affect the estimated activity and shows that RCs can be up to 21% higher in phantoms without plastic walls. A study by Hofheinz et al. (*21*) addresses the effect on the volume-reproducing threshold and shows, for example, that application of a threshold optimized using spheres with walls can lead to an overestimation of volumes by up to 43%. The impact on RCs and estimated volumes can be expected to be even higher for smaller objects imaged with higher resolution.

The aims of this study were to investigate a slightly modified version of a method for the delineation of tumor volume (*7*) and to correct the measured mean activity within the volume for PVE using correction factors (*13*). The aim was to study the effect on small volumes such as lymph nodes and small tumors, and it was therefore of particular interest to evaluate possible improvements when including a modern resolution recovery algorithm in the reconstruction. The corrected results were compared with the mean uptake without correction and with the maximum uptake values. For the purpose of the study, we developed a phantom with active volumes ranging from approximately 0.1 to 0.7 mL (6–11 mm in equivalent diameter). The active volumes were made of balloons having walls that are considerably thinner than those in commercially available phantoms, which is a clear advantage when evaluating PVE. We used standard scanning protocols for head and neck tumors, which is one type of study that can use SUVs in the diagnosis of small tumors and lymph nodes (*22*). However, the methods for tumor delineation and PVE correction are general and could be implemented in the same manner for other studies.

MATERIALS AND METHODS

Phantom

We constructed a phantom using 5 small balloons (Goldbal 3; Balt Extrusion) initially intended for neurointervention. The balloons, which can be seen in Figure 1, were filled to different volumes with an ^{18}F-FDG solution. The volumes were determined using a scale, and the small volumes, which were of interest for PVE correction, ranged from 0.113 to 0.698 mL. The wall thickness of the smallest balloon was estimated to 0.03 mm using the measured weight of the expandable part (3 mg), the estimated

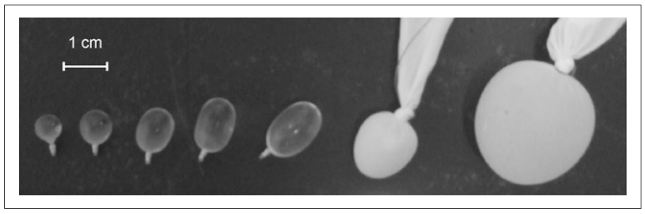

FIGURE 1. All balloons in phantom.

equivalent diameter of 6.0 mm, and the density of Latex (Dow Chemical Co.) (0.92 g/cm^3 (*23*)). Two larger balloons of 1.468 and 9.172 mL were used as references for activity concentration and for optimizing parameters in the volume delineation method. These balloons were made using 2 fingers of a rubber glove, which were filled with an ^{18}F-FDG solution and tied with a knot. The 1.468-mL balloon showed signs of leakage and was hence not included in further analysis. The 5 balloons intended for neurointervention will be referred to as the balloons, and the larger, homemade balloon will be referred to as the reference balloon.

The smallest of the 5 balloons was basically spheric, whereas the larger one was ellipsoidal, with a height and width as defined in Figure 2. An equivalent diameter was calculated as the diameter of a sphere with the measured balloon volume, determined from the scale. Table 1 lists the volume (as measured from the scale), diameter, height, and equivalent diameter of the balloons.

The balloons and the reference balloons, attached to syringes, were mounted to hang from the lid of a plastic box filled with 10 L of a solution of water mixed with ^{18}F-FDG (Fig. 2). The ^{18}F-FDG and water solution, which served as the background, was mixed to a homogeneous activity concentration using a propeller connected to a drilling machine.

Clinical ^{18}F-FDG PET/CT examinations showed that a typical background in the head and neck region of a patient, 1 h after injection of 4 MBq/kg, had an SUV of about 0.7, corresponding to an activity concentration of approximately 2 kBq/mL. By adding activity to the background, we could modify the simulated lesion-to-background activity ratio without refilling the balloons. During the course of the phantom experiment, we kept the same clinically realistic noise level in the background by varying the scan time, taking background activity and radioactive decay into account. The phantom was first imaged with no background activity. The background activity was then gradually increased in 6 steps, giving—in addition to the zero-background measurement—a series

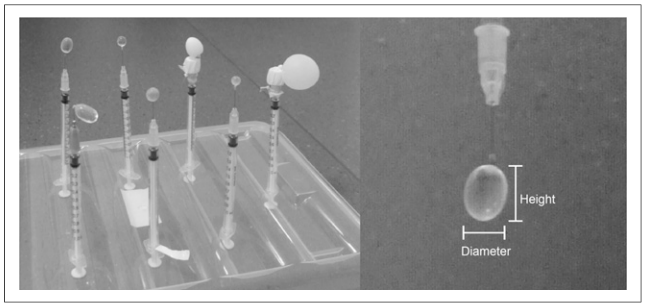

FIGURE 2. Balloons attached to syringes, which are inserted through holes in lid of phantom. When lid is mounted on phantom, syringes hang from top of phantom, with balloons a few centimeters from bottom of box.

TABLE 1
Balloon Volumes and Dimensions

Volume (mL)	Diameter (mm)	Height (mm)	Equivalent diameter (mm)
0.113	6	7	6.0
0.208	7	8	7.4
0.352	8	10	8.8
0.481	8	12	9.7
0.698	10	15	11.0

with balloon-to-background ratios of 14.9, 12.5, 9.1, 6.0, 4.1, and 2.0. The images from the 2.0 ratio measurement, however, were discarded because the balloons were not visible with such a low ratio. The ratios that were used correspond to simulated SUVs in a lesion, ranging from approximately 3 to 10 with a background of approximately 0.7.

Data Acquisition

The PET/CT Discovery 690 (GE Healthcare) scanner at the Nuclear Medicine Department, Umeå University Hospital, was used for image acquisition and reconstruction. The VUE-point HD (VP HD) and SharpIR iterative reconstructions were used as supplied with the scanner. A CT scan was obtained for the purpose of attenuation correction, followed by a dynamic PET scan of 10 equal-length time frames to get 10 measurements of the same data for use with statistical analysis.

The images were reconstructed with 2 different 3-dimensional ordered-subset expectation maximization scatter- and attenuation-correction reconstruction methods, as supplied with the PET/CT scanner. Both methods are routinely used for head and neck ^{18}F-FDG PET/CT patients at Umeå University Hospital. The VUE-point HD (VP HD) reconstruction was applied using 2 iterations, 24 subsets, and a gaussian postprocessing filter of 6.4 mm in FWHM. The SharpIR reconstruction method (*18*), which includes a resolution recovery, was applied using 3 iterations, 24 subsets, and a gaussian postprocessing filter of 3 mm in FWHM. Both reconstructions generated a 50-cm field of view (FOV), 256 × 256 image matrix (1.95 × 1.95 mm pixel size), and slice thickness of 3.27 mm.

To allow for a long experiment time, we started with a relatively high activity concentration of 62 kBq/mL in the balloons. We could therefore reduce the scan time to 2 min per FOV instead of the clinically used 4-min patient scan time per FOV for a head and neck ^{18}F-FDG PET/CT study.

PSF

The method for PVE correction requires knowledge about the PSF, which was measured according to the following procedure. The end of a thin capillary tube was filled with ^{18}F-FDG and served as an approximate point source. Because the PSF is dependent on the position in the PET scanner, the capillary tube was placed at different distances from the origin in the transversal plane (at radii 0, 1, 2, 5, 10, and 15 cm).

The PSF images were reconstructed with the 2 algorithms described in the "Data Acquisition" section, and a 3-dimensional gaussian function was fitted to the result, using the least-squares method. The maximum value in the PSF image was selected, and the vectors in *x, y,* and *z* directions that included the maximum value were used for analysis. For all 3 vectors, the sum of the squared differences between the measured values in each voxel and the integral of the gaussian function over the length of 1 voxel was minimized for varying mean values and FWHMs. The software imlook4d (www.diccom-port.com) and Matlab (The MathWorks, Inc.) was used for the analyses.

All balloons were located within 10 cm of the origin of the FOV, which is also the region in which tumors or lymph nodes typically are found in an ^{18}F-FDG head and neck study. Within this area, we could not find any position dependency of the FWHM; therefore, a mean of the 0- to 10-cm measurements was used for the PVE corrections.

Image Processing

The image processing can be divided into 2 parts: the determination of the volume of each balloon and the PVE correction of the mean activity within the volume.

Several methods for volume delineation have been proposed (*7,24–27*), and we chose a threshold-based method (*7*) that has been shown to yield accurate results (*28*). The threshold, $I_{threshold}$, is calculated as a weighted sum of the balloon and background intensities (I_{mean} and $I_{background}$), as in Equation 1. ε is a weighting factor that will be described below.

$$I_{threshold} = \varepsilon \times I_{mean} + I_{background}. \quad \text{Eq. 1}$$

I_{mean} has been proposed to be calculated as in Equations 2 and 3 (*7,28*), where P_i is the value of voxel i, I_{max} is the maximum voxel value in the balloon, and f_i is the elements in a matrix of the same size as the PET image.

$$f_i = \begin{cases} 1 \; ; \; P_i \geq 0.7 \times I_{max} \\ 0 \; ; \; P \; < 0.7 \times I_{max} \end{cases}. \quad \text{Eq. 2}$$

$$I_{mean} = \frac{1}{\sum_i f_i} \sum_i P_i \times f_i. \quad \text{Eq. 3}$$

In Equation 3, I_{mean} is, however, dependent on the background level. We propose a small change, where the threshold for I_{mean} is proportional to the difference between maximum activity and background activity as in Equations 4 and 5:

$$f'_i = \begin{cases} 1 \; ; P_i \geq 0.7 \times \left(I_{max} - I_{background}\right) + I_{background} \\ 0 \; ; P < 0.7 \times \left(I_{max} - I_{background}\right) + I_{background} \end{cases}. \quad \text{Eq. 4}$$

$$I'_{mean} = \frac{1}{\sum_i f_i} \sum_i P_i \times f'_i. \quad \text{Eq. 5}$$

This gives a threshold that is less dependent on background activity. For $I_{background}$, we used the mean intensity within a manually defined VOI of 4,725 voxels in the constant background volume. ε is a parameter depending on image resolution that needs to be optimized for the scanner and for different image reconstructions (*28*), which are performed by varying ε in steps of 0.025 and selecting the value that yields the VOI size closest to the true volume of the 9.172-mL reference balloon. For each background, the ε corresponding to the most accurate result was selected. The mean value of these ε values, rounded to closest 0.025 step, was then used for all backgrounds.

PVE correction was performed using correction factors, determined with the calculated VOI as a mask, which is convolved

with the system PSF (*5,13*). The idea is that the VOI has the shape of the true uptake, which in PET images is blurred by the PSF. The technique is based on the assumption that the image has 2 homogeneous regions: tumor–balloon and background. Calculating the biases introduced by blurring the VOI will yield the correction factors α and β in Equations 7 and 8 (*5*). α is proportional to the activity left in the VOI after spill-out, and β is proportional to spill-in from the surrounding background. VOI in the equations is a 3-dimensional matrix of the same size as the PET images of the balloons, where all voxels within the active lesion are set to 1 and all other voxels have value of 0. PSF is a matrix of the PSF of the same size as the VOI, and i and j are indices for the voxels in the matrices. ONE is a matrix with every voxel value equal to 1, and ⊗ is the convolution symbol.

$$VOI = \begin{cases} 1 \ ; \ P_i \geq I_{threshold} \\ 0 \ ; \ P_i < I_{threshold} \end{cases}. \quad \text{Eq. 6}$$

$$\alpha = \frac{1}{\sum_i VOI_i} \sum_j (VOI \otimes PSF)_j \times VOI_j. \quad \text{Eq. 7}$$

$$\beta = \frac{1}{\sum_i VOI_i} \sum_j ((ONE - VOI) \otimes PSF)_j \times VOI_j = \\ = \frac{1}{\sum_i VOI_i} \sum_j (ONE - VOI \otimes PSF)_j \times VOI_j = 1 - \alpha. \quad \text{Eq. 8}$$

If I_{total} is the mean activity concentration measured in the balloon in the PET image, $I_{corrected}$ is the real mean activity concentration in the balloon, and $I_{background}$ is the mean activity concentration in the background, the following equation gives the balloon activity (*13*):

$$I_{corrected} = \frac{I_{total} - \beta \times I_{background}}{\alpha}. \quad \text{Eq. 9}$$

Image Analysis

For all 10 frames, for each balloon in each background, we collected the values for uncorrected activity, corrected activity, and the maximum voxel value for the uncorrected volume. The maximum voxel value was included, because this is a common method for measuring SUVs of small objects. All values were divided by the true uptake to enable comparison. The reference balloon was used for determining true uptake, using the mean activity concentration of the 27 innermost voxels in the PET image volume. The 10 frames of the same data were used to calculate means and corresponding SDs. The values were plotted for each background as a function of the volume of each balloon. In addition, the volumes are presented for each background as a plot of the estimated balloon volume as a function of the true volume, determined from weighing the balloons.

RESULTS

Volume Estimation

The weighting factor ε in Equation 1 was determined for the reference balloon in all background levels, and the result can be seen in Table 2. The mean for ε was calculated as 0.35 for VP HD images and 0.275 for SharpIR images. These values were used to determine the volumes of the 5 small balloons. The highest volume error for the largest balloon in the VP HD images using an ε of 0.35 was for the 0 background measurement, where the error is 14% of the true volume. For images reconstructed with SharpIR, using an ε of 0.275 results in a maximum error of 7%, for the background ratio 4.1.

TABLE 2
Optimal Value of ε for All Activity Ratios

Activity ratio	VP HD	SharpIR
4.1	0.300	0.250
6.0	0.325	0.275
9.1	0.350	0.300
12.5	0.375	0.300
14.9	0.375	0.300
No background	0.425	0.275
Mean	0.350	0.275

Mean value is rounded to closest of tested values.

Figure 3 shows a comparison of the methods for defining I_{mean} and I'_{mean} in Equations 3 and 5, respectively. The figure shows that the bias in the estimated volume is smaller for the small balloons when using I'_{mean} instead of I_{mean} in Equations 3 and 5, respectively. The difference between the methods can be seen only for high backgrounds (ratios, 6.0 and 4.1, respectively).

The measured volumes from 3 backgrounds can be seen in Figure 4. According to the figure, volumes as small as 0.35 mL (8.8 mm in equivalent diameter) can be correctly estimated in images reconstructed with SharpIR for a large spread of lesion-to-background ratios. These volumes had corrected means within 1 SD from the true value. The SD increased for lower lesion-to-background ratios. For lesions with lower uptake, the uncertainties are higher and a small object can be mistaken for a larger one. For example, the SDs are always higher for the lesion-to-background ratio of 4.1 than for the ratio of 14.9.

In Figure 4B it can be seen that the volumes determined from the VP HD reconstructions are inferior to those reconstructed using SharpIR. The estimated volumes are far from the true volumes, with an error as high as 100% for the 0.35-mL balloon with a ratio of 14.9. The estimates also depend on the background level, with lower estimated volumes for higher backgrounds.

PVE Correction

The PSF was measured to have a FWHM of 3.2 mm in the radial direction and 4.7 mm in the axial direction for the SharpIR reconstruction. The corresponding values for VP HD are 7.3 mm in the radial direction and 6.1 mm in the axial direction. The differences between the values at different radii from the origin were never larger than 0.3 mm and showed no correlation to positions within a radius of 10 cm. The mean values were used for calculating the correction factors according to Equations 7 and 8.

The results of uncorrected and PVE-corrected activity concentrations within the estimated VOIs are shown in Figure 5, together with the maximum voxel values within the

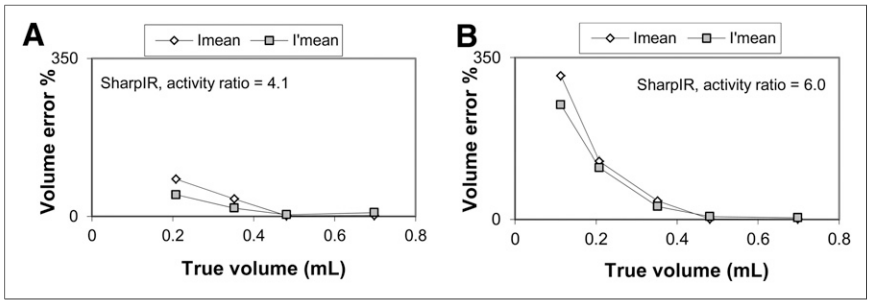

FIGURE 3. Comparison of methods for volume delineation, using either I_{mean} or I'_{mean} in Equation 1. (A) Relative volume error for ratio of 4.1. (B) Corresponding results for ratio of 6.0.

uncorrected VOI. Figure 5 shows that the activity estimates have means within 1 SD from the true values for all balloons larger than 0.35 mL in images reconstructed with SharpIR. For VP HD, the measured relative uptake is far from 1, both before and after partial-volume corrections, as shown in Figure 5. The activity estimates are background-dependent, with lower activity estimates in the balloons with lower backgrounds.

Figure 5 also shows that using the maximum uptake as an activity measure gives an overestimate in images reconstructed with SharpIR. Only a few of the mean maximum values are within 1 SD of the true value. The overestimates vary with balloon size and are as large as 46% for the second largest balloon in Figure 5A. Figure 5 also shows that the SD of the maximum uptake is comparable to, or higher than, the PVE-corrected uptake.

DISCUSSION

We have evaluated methods for delineation and quantification of active volumes smaller than 0.7 mL on images reconstructed with 2 different algorithms. Together, these methods compose a technique for volume delineation and quantification of small active volumes, such as lymph nodes and small tumors. No prior information on lesion size or shape is required.

The phantom developed for this study is useful for studies of PVEs. Most important, it eliminates the effect of plastic walls that most other phantoms have, thus making it more similar to the patient geometry. Compared with this phantom, patient images can be expected to give slightly degraded results due to motion, such as from breathing, although many studies are performed using motion correction (*29–31*). Another difference is that the phantom has a homogeneous activity concentration within both the tumor and the background, which usually is not the case in patient images. For the small lesions considered in this study, the heterogeneities within the lesion in patients should not be too comprehensive. PVE correction of larger heterogeneous tumors will be affected differently, depending on the characteristics of the heterogeneities. If necrosis is present, the necrotic part will not be included in the calculated volume, which is advantageous for this PVE-correction approach. In general, however, heterogeneity will make the estimated volumes less reliable. If the maximum value is collected from a so-called hot spot within the tumor, there is a risk that the calculated threshold is too high to include parts of the tumor with relatively low uptake. Other approaches for calculating thresholds should then be considered. For example, the hot spot can be discarded from the VOI, which is used for determining the maximum value. The case of a heterogeneous background must also be considered, in which case a mean of an ROI or VOI surrounding the tumor could be used.

Figure 4A shows that the limit for reliable volume delineation in images reconstructed with SharpIR is about 0.35 mL. For a spheric volume, this would correspond to a diameter of 8.8 mm, which is approximately 2.7 times the image resolution. Smaller volumes do not have maximum values representative of the uptake (*5*), and the threshold values will therefore be biased. For the same reasons, balloons of these sizes cannot be correctly delineated in images reconstructed with VP HD. The largest balloon, 0.698 mL if it were spheric, would have an equivalent diameter of 11 mm. This diameter is only 1.5 times the image resolution in images reconstructed with VP HD, which is too small for correct volume determination.

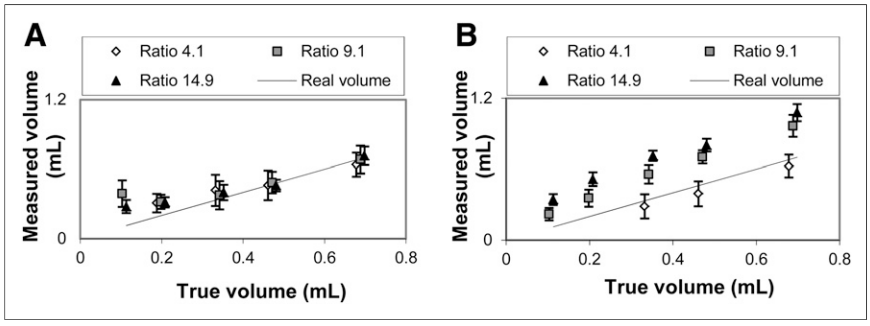

FIGURE 4. Volume estimates for activity ratios of 4.1, 9.1, and 14.9. (A) Results for images reconstructed with SharpIR. (B) Results for images reconstructed with VP HD. Ratios of 4.1 and 9.1 are slightly shifted to left to improve clarity.

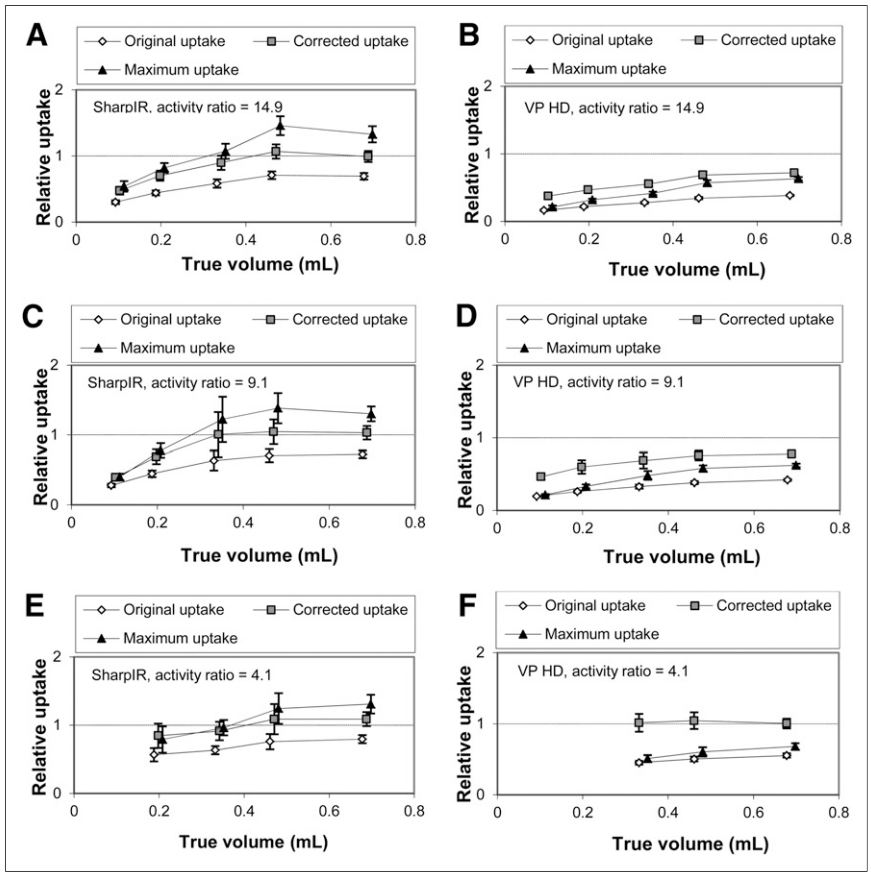

FIGURE 5. Uptake estimates for activity ratios 4.1, 9.1, and 14.9 before and after partial-volume corrections, and compared with maximum uptake value. Original uptake and corrected uptake are shifted slightly to left to improve clarity.

Correct volume delineation is important for the PVE correction, which implies that PVE corrections have fairly accurate results for volumes larger than 0.35 mL in images reconstructed with SharpIR. The results in Figures 5A, 5C, and 5E show lower SDs for higher lesion-to-background ratios but approximately the same means for all ratios. Lower lesion-to-background ratios imply more variation in the results. Because the volumes are incorrectly delineated in images reconstructed with VP HD, the activity estimation is relatively poor. If more accurate volume estimates were available from other imaging modules such as CT or MR, the results would most likely be substantially improved, both for VP HD and for volumes smaller than 0.35 mL using SharpIR.

The method used for PVE correction is fairly sensitive to deviations in the PSF, making accurate measurements crucial. In this study, the objects were positioned in the central part of the FOV. The PSF was found to be fairly constant in this area, and a constant PSF was therefore assumed. If the studied objects are outside the central FOV, it would be recommended to use a spatially varying PSF. The SharpIR algorithm includes correction for spatial variations in the PSF, which should cause a less position-dependent resolution, making the spatially varying PSF a smaller problem, albeit still a problem. Because the image reconstruction algorithms use postfiltering, the largest contribution to the PSF comes from the filter.

The PVE-corrected values in this study are generally more accurate than the maximum values for the VOI and have less statistical variation, thus making this the superior method. Statistical variation is increased, compared with uncorrected values, due to uncertainties in volume delineation, but the mean is substantially more accurate. The method is easily implemented because both lesion delineation and PVE correction can be automated from a maximum value and a background VOI. This automation also makes the method relatively user-independent. The only subjective parameter is the background VOI, which is manually drawn in this study.

A high number of studies have earlier been made on the subject of PVEs (*9,10,19*). However, many of these are performed on phantoms with spheres with relatively thick walls, which reduce effects from background activity. This degradation is small when the FWHM of the PSF is as large as 6–7 mm but increases substantially with an FWHM of 3–4 mm in the case of one of the reconstruction algorithms evaluated in this study. Most studies are also made with spheres larger than 10 mm in diameter, which is fairly large, compared with the resolution using modern algorithms for image reconstruction.

CONCLUSION

The tested method for volume delineation gives accurate estimates of volumes of active lesions of 0.35 mL and larger

on images reconstructed with a modern resolution recovery method. These lesions could also be correctly quantified in terms of activity. Images reconstructed without resolution recovery were not appropriate for volume delineation and thereby not for activity quantification of the small lesions in this study. The results further support implementation of resolution recovery methods in PET imaging.

DISCLOSURE

This study was jointly supported by the Swedish Cancer Society, Lion's Cancer Research Foundation, Umeå University, the Faculty of Medicine at Umeå University, and the University Hospital of Umeå. No other potential conflict of interest relevant to this article was reported.

REFERENCES

1. Poeppel TD, Krause BJ, Heusner TA, Boy C, Bockisch A, Antoch G. PET/CT for the staging and follow-up of patients with malignancies. *Eur J Radiol.* 2009;70:382–392.
2. Hoekstra CJ, Paglianiti I, Hoekstra OS, et al. Monitoring response to therapy in cancer using [^{18}F]-2-fluoro-2-deoxy-D-glucose and positron emission tomography: an overview of different analytical methods. *Eur J Nucl Med.* 2000;27:731–743.
3. Basu S, Alavi A. Partial volume correction of standardized uptake values and the dual time point in FDG-PET imaging: should these be routinely employed in assessing patients with cancer? *Eur J Nucl Med Mol Imaging.* 2007;34:1527–1529.
4. Huang SC. Anatomy of SUV. *Nucl Med Biol.* 2000;27:643–646.
5. Soret M, Bacharach SL, Buvat I. Partial-volume effect in PET tumor imaging. *J Nucl Med.* 2007;48:932–945.
6. Hoffman EJ, Huang SC, Phelps ME. Quantitation in positron emission computed tomography: 1. Effect of object size. *J Comput Assist Tomogr.* 1979;3:299–308.
7. Nestle U, Kremp S, Schaefer-Schuler A, Sebastian-Welsch C, Hellwig D, Rübe C. Comparison of different methods for delineation of ^{18}F-FDG PET: positive tissue for target volume definition in radiotherapy of patients with non–small cell lung cancer. *J Nucl Med.* 2005;46:1342–1348.
8. Pelosi E, Billè A, Skanjeti A, et al. Prognostic role of the PET parameter maximum standardized uptake value in non-small cell lung cancer: analysis in tumour of diameter $\geq$ and $<$25 mm. *Q J Nucl Med Mol Imaging.* 2011;55:72–80.
9. Hoetjes NJ, van Velden FH, Hoekstra OS, et al. Partial volume correction strategies for quantitative FDG PET in oncology. *Eur J Nucl Med Mol Imaging.* 2010;37:1679–1687.
10. Teo BK, Seo Y, Bacharach SL, et al. Partial-volume correction in PET: validation of an iterative postreconstruction method with phantom and patient data. *J Nucl Med.* 2007;48:802–810.
11. Hofheinz F, Langner J, Petr J, et al. A method for model-free partial volume correction in oncological PET. *EJNMMI Res.* 2012;2:16.
12. Erlandsson K, Buvat I, Pretorius PH, Thomas BA, Hutton BF. A review of partial volume correction techniques for emission tomography and their applications in neurology, cardiology and oncology. *Phys Med Biol.* 2012;57:R119–159.
13. Geworski L, Knoop BO, Cabrejas MLD, Knapp WH, Munz DL. Recovery correction for quantitation in emission tomography: a feasibility study. *Eur J Nucl Med.* 2000;27:161–169.
14. Haug AR, Tiega Donfack BP, Trumm C, et al. ^{18}F-FDG PET/CT predicts survival after radioembolization of hepatic metastases from breast cancer. *J Nucl Med.* 2012;53:371–377.
15. Keam B, Im AS, Koh Y, et al. Predictive value of FDG PET/CT for pathologic axillary node involvement after neoadjuvant chemotherapy. *Breast Cancer.* 2013; 20:167–173.
16. Carkaci S, Adrada BE, Rohren E, et al. Semiquantitative analysis of maximum standardized uptake values of regional lymph nodes in inflammatory breast cancer: is there a reliable threshold for differentiating benign from malignant? *Acad Radiol.* 2012;19:535–541.
17. Boellaard R, Krak NC, Hoekstra OS, Lammertsma AA. Effects of noise, image resolution, and ROI definition on the accuracy of standard uptake values: a simulation study. *J Nucl Med.* 2004;45:1519–1527.
18. Bettinardi V, Presotto L, Rapisarda E, Picchio M, Gianolli L, Gilardi MC. Physical performance of the new hybrid PET/CT Discovery-690. *Med Phys.* 2011;38: 5394–5411.
19. Boussion N, Cheze Le Rest C, Hatt M, Visvikis D. Incorporation of wavelet-based denoising in iterative deconvolution for partial volume correction in whole-body PET imaging. *Eur J Nucl Med Mol Imaging.* 2009;36:1064–1075.
20. Bazañez-Borgert M, Bundschuh RA, Herz M, Martinez MJ, Schwaiger M, Ziegler SI. Radioactive spheres without inactive wall for lesion simulation in PET. *Z Med Phys.* 2008;18:37–42.
21. Hofheinz F, Dittrich S, Pötzsch C, Hoff J. Effects of cold sphere walls in PET phantom measurements on the volume reproducing threshold. *Phys Med Biol.* 2010;55:1099–1113.
22. Kubicek GJ, Champ C, Fogh S, et al. FDG-PET staging and importance of lymph node SUV in head and neck cancer. *Head Neck Oncol.* 2010;2:1–7.
23. Nordling C, Österman J. *Physics Handbook for Science and Engineering*. Lund, Sweden: Studentliteratur; 2006:33
24. Erdi YE, Mawlawi O, Larson SM, et al. Segmentation of lung lesion volume by adaptive positron emission tomography image thresholding. *Cancer.* 1997;80: 2505–2509.
25. Daisne JF, Sibomana M, Bol A, Doumont T, Lonneux M, Grégoire V. Tridimensional automatic segmentation of PET volumes based on measured source-to-background ratios: influence of reconstruction algorithms. *Radiother Oncol.* 2003;69:247–250.
26. Black QC, Grills IS, Kestin LL, et al. Defining a radiotherapy target with positron emission tomography. *Int J Radiat Oncol Biol Phys.* 2004;60: 1272–1282.
27. Schaefer A, Kremp S, Hellwig D, Rübe C, Kirsch CM, Nestle U. A contrast-oriented algorithm for FDG-PET-based delineation of tumour volumes for the radiotherapy of lung cancer: derivation from phantom measurements and validation in patient data. *Eur J Nucl Med Mol Imaging.* 2008;35: 1989–1999.
28. Tylski P, Stute S, Grotus N, et al. Comparative assessment of methods for estimating tumor volume and standardized uptake value in ^{18}F-FDG PET. *J Nucl Med.* 2010;51:268–276.
29. Keller SH, Sibomana M, Olesen OV, et al. Methods for motion correction evaluation using ^{18}F-FDG human brain scans on a high-resolution PET scanner. *J Nucl Med.* 2012;53:495–504.
30. Lucignani G. Respiratory and cardiac motion correction with 4D PET imaging: shooting at moving targets. *Eur J Nucl Med Mol Imaging.* 2009;36:315–319.
31. Liu C, Alessio AM, Kinahan PE. Respiratory motion correction for quantitative PET/CT using all detected events with internal-external motion correlation. *Med Phys.* 2011;38:2715–2723.